COMPUTATIONAL STUDY OF TRACE ELEMENT PARTITIONING BETWEEN ORTHOPYROXENE AND MELT: IMPLICATIONS FOR SUBSTITUTION MECHANISMS IN EARTH AND MOON. M van Kan Parker[1], W. van Westrenen[1], J van Sijl[1]. [1]Faculty of Earth and Life Sciences, VU University Amsterdam, The Netherlands, e-mail: Mirjam.van.kan@falw.vu.nl

Introduction: Orthopyroxene (opx) is a common rock-forming silicate in the Earth's crust and upper mantle, and a major constituent of the Moon's mantle. It played an important role during lunar magma ocean crystallisation, subsequent mantle overturn, and mare basalt formation [1, 2]. Geochemical models of magma ocean crystallisation and later remelting require an understanding of trace element incorporation into the opx structure in the presence of silicate melt.

Trace element partitioning between coexisting equilibrium phases is dependent on pressure (P), temperature (T) and composition (x). Systematic experimental studies of opx-melt partitioning are rare and cover a limited P-T-x range. As a result, no predictive thermodynamic model is available for opx-melt partitioning as there is for clinopyroxene or garnet [3,4], hindering quantitative petrogenetic modelling of lunar rocks. The only predictive model available is purely empirical [5], making extrapolation to conditions outside of the experimental range difficult.

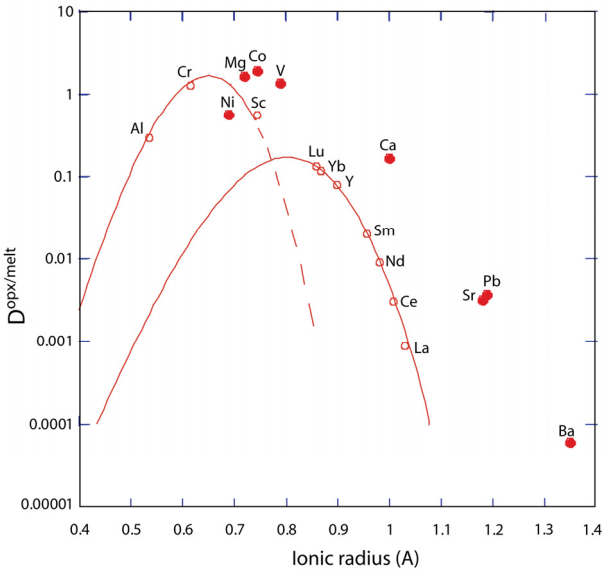

Figure 1. Symbols show experimentally determined $D^{opx/melt}$ values for 2^+ (solid) and 3^+ (open) cations as a function of effective ionic radii in opx at P = 2.7 GPa and T = 1783 K [6]. Two curves are fits to 3^+ data using lattice strain model of [7]: M1 lattice site upper curve, M2 lower curve.

Recently Frei and co-workers [6] studied partitioning of 28 trace elements between opx and anhydrous silicate melt with P = 1.1-3.2 GPa and T = 1503-1803 K experimentally. They use lattice strain theory [7] to rationalise their results and show that trivalent elements (Al, Cr, Sc, REE) have a clear preference for incorporation into the M1 or M2 opx lattice sites, depending on their ionic radius (Fig. 1). The resulting 'ideal radii' for trivalent cations incorporated in opx are 0.65-0.66 Å for the M1 and 0.82-0.85 Å for the M2 site, dependent on P-T conditions [6]. These recent data significantly expand the data set available for constructing a thermodynamics-based predictive partitioning model. However, experiments were performed in Fe-free systems, casting doubt on their applicability to comparatively Fe-rich lunar compositions. To complement the experimental data, assessing the potential role of iron, and to elucidate atomic-scale processes underlying opx-melt partitioning, we performed computer simulations of divalent (2^+) and trivalent (3^+) element partitioning between opx end-members enstatite ($MgSiO_3$), ferrosilite ($FeSiO_3$) and silicate melt.

Methods: Computer simulated mineral-melt trace element partitioning for enstatite and ferrosilite was carried out using static (T= 0 K) lattice energy calculations using GULP [8,9]. We assume crystallisation of the opx end-members in the orthorhombic (*Pbca*) crystal structure. The cations in the M1 and M2 lattice sites are six-fold coordinated with oxygen.

Account is taken for the influence of melt during mineral-melt cation exchange by calculating so-called solution energies [9]. For example, in the case of enstatite-melt equilibration for a random 2^+ trace element J^{2+} entering the M1 site the reaction evaluated is:

$JO(l) + MgMgSi_2O_6(s) \rightarrow MgJSi_2O_6(s) + MgO(l)$ *(1)*

where (l) stands for liquid and (s) for solid. The corresponding solution energy (U_{sol}) is evaluated through:

$U_{sol} = U_{def,f(MgJSi2O6)} + U_{lat(MgO)} - U_{lat(JO)}$ *(2)*

with $U_{def,f}$ being the final defect energy and U_{lat} the lattice energy of the oxide. To interpret the computational results we use Brice's equation [10] relating solution energy to lattice strain energy, which in turn depends on the ideal radius and apparent elasticity of the site on which substitutions take place:

$$U_{strain} = 4\pi E N_A \left[\frac{1}{2} r_0 (r_i - r_0)^2 + \frac{1}{3} (r_i - r_0)^3 \right] \quad (3)$$

where N_A is Avogadro's number, r_0 the optimum radius of the lattice site, r_i the radius of the substituent cation and E the apparent site Young's modulus. Homo- and heterovalent substitutions on the M1 and M2 sites were simulated to enable comparison with the

latest experimental results [6] (Fig. 1). In the homovalent case, a 2^+ trace atom was inserted to replace a Mg or Fe atom, dependent on the studied end-member. For heterovalent substitutions of 3^+ trace elements, two charge balancing mechanisms were evaluated. We assessed (1) two 3^+ atoms replacing a Mg/Fe atom and a tetrahedrally coordinated Si atom (2) a 3^+ atom and a 1^+ atom substituting for two Mg/Fe atoms. In the coupled 3^+ case, the atom replacing Si is Al. For the coupled 1^+ and 3^+ case the 1^+ atom is Li.

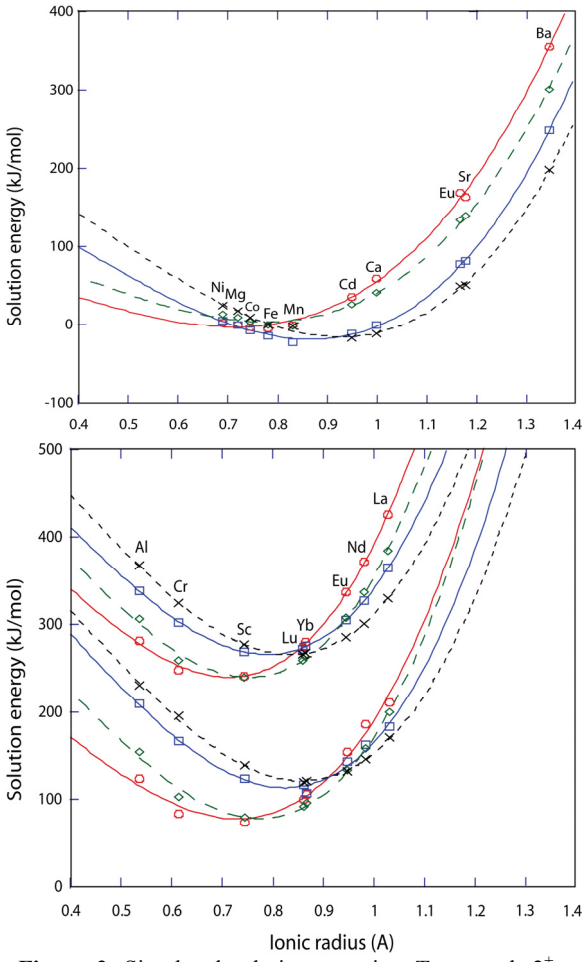

Figure 2. Simulated solution energies: Top panel: 2^+ trace element substitutions in enstatite (solid curves) and ferrosilite (dashed curves). Circles and diamonds represent the M1 lattice site, squares and crosses the M2 site. Bottom panel: coupled 3^+ substitution (top set) and coupled 1^+ and 3^+ substitution (bottom set), curves and symbols are as in top panel.

Results: Substitutions show lower solution energies for 2+ elements than for 3^+ elements of the same radius (Fig. 2), indicating that 2^+ elements are more compatible in opx than 3^+ elements, consistent with experiments (Fig. 1). The simulated optimum ionic radii, r_0, for 2^+ substitutions within enstatite at the M1 and M2 sites are 0.712 and 0.867 Å. Values are significantly higher for ferrosilite (0.775 and 0.926 Å), consistent with the larger size of the Fe^{2+} atom compared to Mg^{2+}.

Optimum radii for the coupled 3^+ substitutions are 0.714 (M1) and 0.790 Å (M2) for enstatite, and about 0.04 Å larger for ferrosilite. Finally M1 and M2 r_0 values for the coupled 1^+ and 3^+ substitution are 0.729 (M1) and 0.824 Å (M2) for enstatite, and 0.774 (M1) and 0.860 Å (M2) for ferrosilite.

The computationally derived r_0 values for the Fe-free system are in good agreement with experimental data (Fig. 1). If variations in r_0 (0.04-0.05 Å) as a function of iron content are as large as predicted in our simulations they will be detectable in future partitioning experiments in Fe-bearing systems.

Fitted apparent Youngs moduli *E* values are significantly lower for the 2^+ (204-255 GPa) compared to the 3^+ substitutions (475-531 GPa) in both enstatite and ferrosilite. This implies that the lattice resists deformation more and points to smaller differences in D values between large and small 2^+ elements compared to large and small 3^+ elements, consistent with experiments (Fig. 1). Young's modulus is largely independent of opx iron content in our simulations.

Conclusions: Our results, specifically the optimum ionic radii in Fe-free systems are in close agreement with the recently determined experimental values [6].

Computer simulations show, similar to experiments, that there is a clear difference in optimum radius of the smaller M1 and larger M2 site. The optimum M1 and M2 radii of ferrosilite are predicted to be significantly larger than those of enstatite. Finally, we show that coupled $1^+/3^+$ substitutions are preferred to coupled 3^+ subsitutions, indicating that the often proposed Al-Si subsitution is less important in opx-melt systems than commonly assumed [11].

The next step in this study is to test theory with experiments in the Na_2O-CaO-FeO-MgO-Al_2O_3-SiO_2 (NCFMAS) sytem, to quantify variations in effective ionic radii as a function of iron content – a key step towards deriving opx-melt partition coefficients applicable to lunar modelling.

References: [1] Taylor and Jake (1974) *GCA 2,* 1287-1305 [2] Snyder et al. (1992) *GCA 56,* 3809-3823 [3] Blundy and Wood (1997) *CMP 129*, 166-181 [4] van Westrenen and Draper, (2007) *CMP 154,* 717-730 [5] Bedard (2007) *Chem Geol 244*, 263-303.[6] Frei et al. (2008) *CMP* [7] Blundy and Wood (1994) *Nature 372*, 452-454 [8] Gale (1997) *Far Trans 93,* 629 [9] van Westrenen et al. (2000) *GCA 64,* 1629-1639 [10] Brice (1975) *J Crys Growth 28,* 249-253 [11] Cameron and Papike (1981) *Am Min 66*, 1-50